

# Magnetic ordering in a model Mott-insulator–band-insulator heterostructure

Satoshi Okamoto\* and Andrew J. Millis

Department of Physics, Columbia University, 538 West 120th Street, New York, New York 10027, USA

(Dated: January 26, 2020)

The magnetic phase diagram of Mott-insulator–band-insulator heterostructures is investigated using the dynamical-mean-field method. It is found that magnetic orderings in the thin heterostructures differ from those in bulk. A ferromagnetic phase is found in the strong coupling regime, and the magnetic moment is seen to be confined at the interface between the two insulators. A bulk-like antiferromagnetic phase is found for the thick heterostructures, but the moment becomes small at the surface and ferromagnetic correlation may characterize the surface layers. Predictions are made for the photoemission experiment and the magnetic transition temperatures as functions of interaction strength and layer thickness.

PACS numbers: 73.20.-r, 71.27.+a, 75.70.-i

Fabrication and investigation of heterostructures involving correlated-electron materials [1, 2] are an important direction in material science. Understanding of the electronic properties near the interfaces and surfaces is not only of scientific interest but is also indispensable to realize electronic devices exploiting the unique properties of correlated-electron materials. A variety of heterostructures have been fabricated and studied including high- $T_c$  cuprates [3, 4], Mott-insulator and band-insulator heterostructure [5], and superlattices of transition-metal oxides [6, 7, 8]. Interestingly, the heterostructures comprising of a Mott-insulator and a band-insulator were reported to show metallic behavior [5].

A fundamental question raised by those studies is “what electronic phases are realized at interfaces.” For the vacuum-bulk interface (i.e., the surface), Potthoff and Nolting [9], Schwieger *et al.* [10], and Liebsch [11] have argued that the reduced coordination may enhance correlation effects. The enhanced correlations could presumably induce surface magnetic ordering, although this possibility was not discussed in Refs. [9, 10, 11]. Matzdorf *et al.* proposed that ferromagnetic ordering is stabilized at the surface of two-dimensional ruthenates by a lattice distortion [12], but this is not yet observed. Surface ferromagnetism had been also discussed in a mean field treatment of the Hubbard model by Potthoff and Nolting [13]. Similarly, the effect of bulk strain on the magnetic ordering in perovskite manganites was discussed by Fang *et al.* [14].

All these studies dealt with systems in which charge densities remain unchanged from the bulk values, and physics arising from the modulation of charge density was not addressed. In this paper, we use the dynamical-mean-field method [15] to establish the phase diagram as a function of geometry, temperature, and interaction for theoretical models which capture the essence of experimentally studied heterostructures, where charge spreading is the fundamental new effect. Our results constitute a significant improvement over previous Hartree-Fock (HF) studies [16], enabling reasonable estimates of transition temperatures and providing new insights into

the spatial variation of the order parameter, establishing that the ferromagnetism is a interface phenomena. We also present theoretical prediction for observables such as single-particle spectral functions.

We study a model heterostructure introduced in Ref. [17]. The Hamiltonian is a simplified representation of the systems studied in Ref. [5] with the orbital degeneracy neglected. We consider [001] heterostructures formed by varying the  $A$ -site of a  $ABO_3$  perovskite lattice. The electrons of interest reside on the  $B$ -site ions, which form a simple cubic lattice with sites labeled by  $i$  as  $\vec{r}_i = (x_i, y_i, z_i) = a(n_i, m_i, l_i)$  with the lattice constant  $a$  set to unity. We assume each  $B$ -site has a single orbital; electrons hop between nearest neighbor sites with the transfer  $t$ . The electrons interact via a on-site interaction  $U$  and a long-ranged Coulomb repulsion. The heterostructure is defined by  $n$  planes of charge +1 counterions placed on the  $A'$  sublattice of  $A$ -site ions at positions  $\vec{r}_j^{A'} = a(n_j + 1/2, m_j + 1/2, l_j + 1/2)$ , with  $-\infty < n_j, m_j < \infty$  and  $l_j = 1, \dots, n$ . The resulting Hamiltonian is  $H = H_{band} + H_{int} + H_{Coul}$  with

$$H_{band} = -t \sum_{\langle ij \rangle, \sigma} (d_{i\sigma}^\dagger d_{j\sigma} + H.c.), \quad (1)$$

$$H_{int} = U \sum_i n_{i\uparrow} n_{i\downarrow} + \frac{1}{2} \sum_{\substack{i \neq j \\ \sigma, \sigma'}} \frac{e^2 n_{i\sigma} n_{j\sigma'}}{\varepsilon |\vec{r}_i - \vec{r}_j|}, \quad (2)$$

$$H_{Coul} = - \sum_{i,j,\sigma} \frac{e^2 n_{i\sigma}}{\varepsilon |\vec{r}_i - \vec{r}_j^{A'}|}. \quad (3)$$

Note that  $U \neq 0$  on all sites. Charge neutrality requires that the areal density of electrons is  $n$ . A dimensionless measure of the strength of the long-ranged Coulomb interaction is  $E_c = e^2/(\varepsilon a t)$  with the dielectric constant  $\varepsilon$ . In the most of our analysis, we choose  $E_c = 0.8$ . This corresponds to  $t \sim 0.3$  eV,  $a \sim 4$  Å, and  $\varepsilon = 15$ , which describe the system studied in Ref. [5]. The charge profile is found not to depend in an important way on  $\varepsilon$ , but the stability of magnetic orderings does because this is sensitive to the details of the charge density distribution

as discussed later.

The basic object of our study is the electron Green's function. In general, this is given by

$$G_\sigma(\vec{r}, \vec{r}'; \omega) = [\omega + \mu - H_{band} - H_{Coul} - \Sigma_\sigma(\vec{r}, \vec{r}'; \omega)]^{-1}, \quad (4)$$

with the chemical potential  $\mu$  and the electron self-energy  $\Sigma$ . We consider [001] heterostructures with either in-plane translational invariance or  $N_s$ -sublattice antiferromagnetism. The Green's function and self-energy are therefore functions of the variables  $(z, \eta, z', \eta', \vec{k}_\parallel)$  where  $\eta$  and  $\eta' (= 1, \dots, N_s)$  label the sublattice in layers  $z$  and  $z'$ , respectively, and  $\vec{k}_\parallel$  is a momentum in the (reduced) Brillouin zone. As in Ref. [17], we approximate the self-energy as the sum of a static Hartree term  $\Sigma_\sigma^H$  arising from the long-ranged part of the Coulomb interaction and a dynamical part  $\Sigma_\sigma^D(\omega)$  arising from local fluctuations. Generalizing the inhomogeneous case of the dynamical-mean-field theory (DMFT) [10], we assume that the self-energy is only dependent on layer  $z$  and sublattice  $\eta$ . Thus, the dynamical part of the self-energy is written as

$$\Sigma_\sigma^D \Rightarrow \Sigma_\sigma^D(z, \eta; \omega). \quad (5)$$

The  $z\eta$ -dependent self-energy is determined from the solution of a quantum impurity model [15] with the mean-field function fixed by the self-consistency condition

$$G_\sigma^{imp}(z, \eta; \omega) = N_s \int \frac{d^2 k_\parallel}{(2\pi)^2} G_\sigma(z, \eta, z, \eta, \vec{k}_\parallel; \omega). \quad (6)$$

In general for the heterostructure with  $L$  layers with  $N_s$  sublattices, one must solve  $L \times N_s$  independent impurity models. Due to the self-consistency condition [cf. Eq. (6)] and to compute the charge density  $n_\sigma(z, \eta) = -\int \frac{d\omega}{\pi} f(\omega) \text{Im} G_\sigma^{imp}(z, \eta; \omega)$  with  $f$  the Fermi distribution function, it is required to invert the  $(L \times N_s)^2$  Green's function matrix at each momenta and frequency. This time consuming numerics restricts the size of the unit cell. In this study, we consider the commensurate magnetic states with up to two sublattices,  $N_s = 1$  and  $2$ , on each layer and with the charge density independent of the sublattices, i.e., paramagnetic (PM), ferromagnetic (FM) states, and (layer-) antiferromagnetic (AF) state where antiferromagnetic (FM) planes with moment alternating from plane to plane. Note that the AF state extrapolates to the bulk AF state with the magnetic vector  $\vec{q} = (\pi, \pi, \pi)$  at  $n \rightarrow \infty$ . By symmetry, the number of quantum impurity models one must solve is reduced to  $L$ . However, solution of the impurity models is a time consuming task, and an inexpensive solver is required. In Ref. [17], to study the evolution of the low-energy quasiparticle band and high-energy Hubbard bands as a function of position, we applied two-site DMFT [18] which is a simplified version of exact-diagonalization method. At  $T = 0$ , this method is known to give reasonable result for

Mott metal-insulator and magnetic transitions. However, small number of bath orbitals is known to be insufficient to describe the thermodynamics correctly [19].

In order to investigate the magnetic behavior at finite temperature, we apply semiclassical approximation (SCA) [19]. In this approximation, two continuous Hubbard-Stratonovich transformations are introduced, coupling to spin- and charge-fields. When evaluating the partition function, only spin-fields at zero-Matsubara frequency are kept and saddle-point approximation is applied for charge-fields at given values of spin-fields. This method is found to be reasonably accurate to compute magnetic transition temperature because, in most of the correlated electron systems, very slow spin-fluctuation becomes dominant near the magnetic transition. In contrast to the two-site DMFT, the SCA can not reproduce quasiparticle peak at  $\omega = 0$ . This is due to the neglect of quantum fluctuation of Hubbard-Stratonovich fields in the SCA. However, the SCA reproduces the spectral function in paramagnetic phase at not-too-low temperature and in the strong coupling regime, and in the magnetically ordered phase.

First, we investigate the magnetic behavior at finite temperature. The upper panel of Fig. 1 shows our calculated phase diagram in the interaction-temperature plane for heterostructures with various thicknesses. The one-layer heterostructure is PM at weak to moderate interactions, and FM at strong interactions. The two- and three-layer heterostructures are AF at weak to intermediate interaction, and become FM at stronger interactions with almost the same  $T_C$  for  $n = 2$  and  $3$ . The phase diagram displays regions where both  $T_C$  and  $T_N > 0$  (FM and AF both locally stable); in these regions the phase with the higher transition temperature has the lower free energy and is the one which actually occurs. As will be shown below, the ferromagnetism is an interface effect. We expect that at large  $U$ , very thick heterostructures will be AF in the center, but with a FM surface layer. Antiferromagnetic Néel temperature  $T_N$  is found to be strongly dependent on the layer thickness; it increases with the increase of layer thickness. Note that  $T_N$ 's are substantially reduced from the bulk value ( $T_N^{max}/t \sim 0.47$  at  $U/t \sim 10$ ) due to the smaller charge density per site. Hartree-Fock studies of this and related models find a layer-AF phase. This phase is not found in our DMFT analysis.

The lower panel of Fig. 1 presents a detailed study of the  $n = 2$  heterostructure showing how changes in the charge confinement parameter  $E_c$  affect the physics. The filled and open points (left-hand axis) show the variation of the Curie and Néel temperatures, respectively. The light solid and light broken lines (right-hand axis) show the variation of charge density on the central and next to central layers, respectively. It is seen that the AF ordering is rapidly destabilized with the decrease of  $E_c$ , and is preempted by the FM ordering. The reduction of

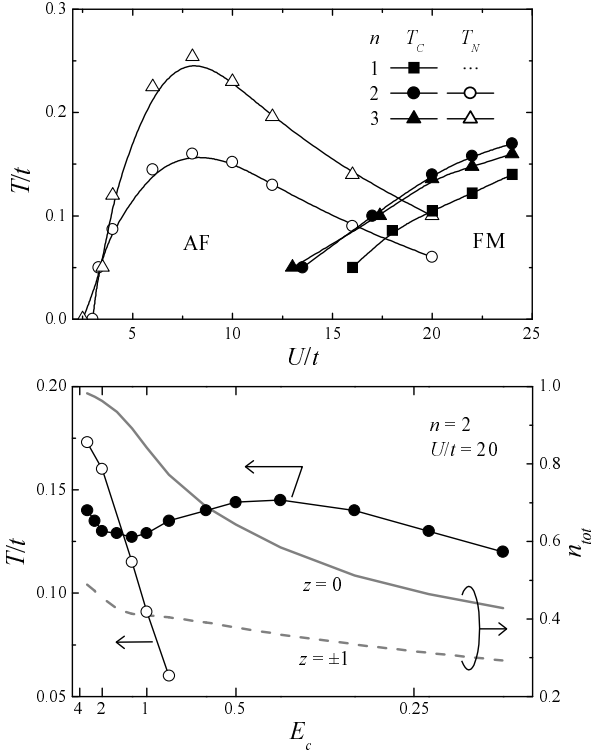


FIG. 1: Upper panel: Magnetic transition temperatures of heterostructures with various thicknesses  $n$  indicated as functions of interaction strength.  $E_c = 0.8$ . Filled symbols: Ferromagnetic Curie temperature  $T_C$ , open symbols: Antiferromagnetic Néel temperature  $T_N$ . Note that, where both phases are locally stable, the phase with higher  $T_C$  ( $T_N$ ) has the lower free energy. Lower panel: Magnetic transition temperatures and charge density  $n_{tot}$  at  $z = 0$  (light solid line) and  $\pm 1$  (light broken line) at  $T/t = 0.1$  as functions of the parameter  $E_c$  for 2-layer heterostructure with  $U/t = 20$ . Counterions are placed at  $z = \pm 0.5$ .

$T_N$  is seen to be correlated to that of the charge density at  $z = 0$ . On the contrary,  $T_C$  has a weak variation with  $E_c$ . This indicates that the FM ordering is favored by the intermediate charge density as discussed in the bulk single-band Hubbard model [20]; at large  $E_c$ , the magnetization is large on the outer layer and small in the inner layer, at small  $E_c$ , the situation is reversed.

We now turn to the spatial variation of the magnetization density. As examples, numerical results for a 4-layer heterostructure with counterions at  $z = \pm 0.5$  and  $\pm 1.5$ , and  $E_c = 0.8$  are presented in Fig. 2. The upper panel of Fig. 2 shows the magnetization in the FM state. In DMFT (filled circles), only the layers near the interfaces ( $|z| \sim 2$ ) have large polarization and inner layers in the heterostructure have small moments. This explains the weak  $n$ -dependence of  $T_C$  of thick heterostructures (see the upper panel of Fig. 1). In HF (open circles), all layers in the heterostructure are highly polarized. In contrast in an AF state, result of the in-plane staggered magnetization by DMFT and HF agree well as shown in the

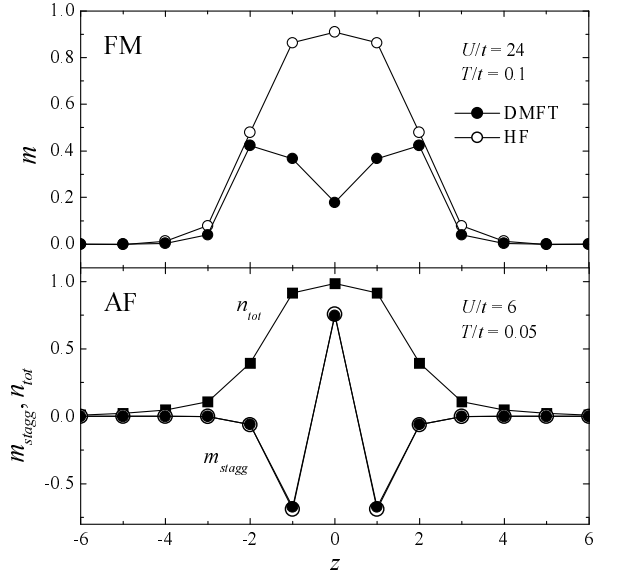


FIG. 2: Magnetization density of 4-layer heterostructure. Counterions are placed at  $z = \pm 0.5, \pm 1.5$ .  $E_c = 0.8$ . Upper panel: Magnetization  $m$  in a FM state for  $U/t = 24$  and  $T/t = 0.1$ . Lower panel: In-plane staggered magnetization  $m_{stagg}$  in an AF state for  $U/t = 6$  and  $T/t = 0.05$ . Filled (open) circles are the results by DMFT (HF). For comparison, charge density  $n_{tot}$  computed by DMFT is also shown in the lower panel (filled squares). Note that the staggered magnetization in the outer layers ( $|z| \geq 2$ ), and the outermost layers ( $|z| = 1$ ) have the same sign.

lower panel of Fig. 2. For comparison, the total charge density is also plotted (filled squares). The in-plane staggered magnetization is large only at inner layers where the charge density is close to 1. Note that the staggered magnetization in the outer layers ( $|z| \geq 2$ ) has the same sign as in the outermost layers ( $|z| = 1$ ) indicating that the outer layers are not intrinsically magnetic.

Spin distributions presented in Fig. 2 can be understood from the single-particle spectral functions. In Fig. 3 are presented the DMFT results for the layer- and sublattice-resolved spectral functions  $A_\sigma(z, \eta; \omega) = -\frac{1}{\pi} \text{Im} G_\sigma^{imp}(z, \eta; \omega + i0^+)$  for the FM (upper panel) and the AF (lower panel) states of 4-layer heterostructure with the same parameters as in Fig. 2. These quantities can in principle be measured by spin-dependent photoemission or scanning tunneling microscopy. As noticed in Ref. [17], spectral function outside of the heterostructure ( $|z| \gg 2$ ) is essentially identical to that of the free tight-binding model  $H_{band}$ , and electron density is negligibly small. With approaching the interfaces ( $|z| = 2$ ), the spectral function shifts downwards and begins to broaden. In the FM case, magnetic ordering is possible only near the interface ( $|z| \sim 2$ ) carrying the intermediate charge density. Inside the heterostructure ( $|z| < 2$ ), clear Hubbard gap exists due to the large  $U$  and uniform polarization is hard to achieve. On the contrary,

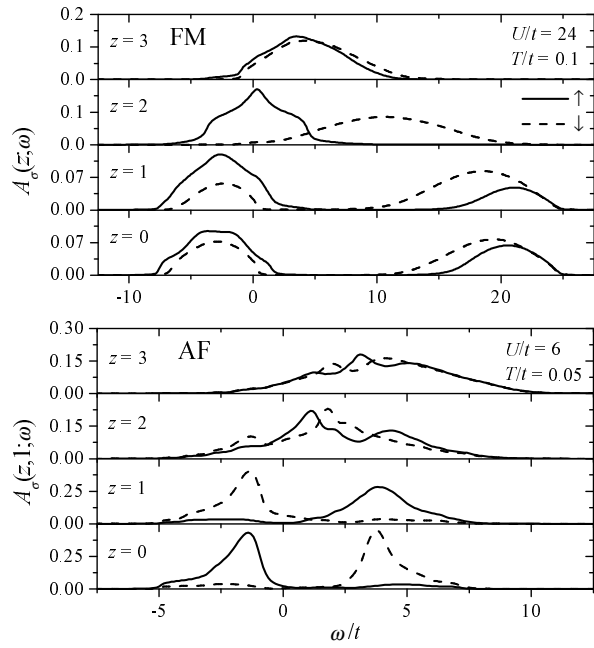


FIG. 3: Layer- and sublattice-resolved spectral functions as functions of real frequency  $\omega$  for 4-layer heterostructure.  $E_c = 0.8$ . Upper panel: Ferromagnetic state at  $U/t = 24$  and  $T/t = 0.1$ . Lower panel: Antiferromagnetic state at  $U/t = 6$  and  $T/t = 0.05$ . Sublattice  $\eta = 1$ . Solid (broken) lines are for up (down) spin electrons. For sublattice  $\eta = 2$  in AF state, up and down electrons are interchanged.

high charge density is necessary to keep the staggered magnetization in the AF case as seen as a difference between up and down spectra in the lower panel of Fig. 3.

In the previous study, we have found an approximately three-unit-cell-wide edge region where the charge density  $n_{tot}$  drops from  $\sim 1$  corresponding to Mott insulating material to  $\sim 0$  corresponding to band insulating one [16, 17]. From the present work, the edge region is found to be FM when the on-site interaction is substantially strong. Critical interaction below which FM state becomes unstable against PM state is  $U_c \sim 13t$ . For very thick heterostructure, it may be possible that the central layers exhibit bulk-like AF ordering while the edge layers exhibit FM ordering. This remains to be investigated in the present framework.

To summarize, we have presented a DMFT study of magnetic behavior of a model Mott-insulator–band-insulator heterostructure in which the behavior is controlled by the spreading of the electronic charge out of the confinement region. Magnetic phase diagram is determined as a function of layer thickness, temperature, and interaction strength. Ferromagnetic Curie temperature is found to be less sensitive to the layer thickness and charge distribution, while AF Néel temperature is sensitive to those parameters. The magnetization in the FM phase is confined to the interface, where the charge density drops from  $\sim 1$  characterizing the Mott-insulator to

$\sim 0$  the band-insulator. Antiferromagnetism appears in heterostructures which are thick enough to exhibit central region with bulk-like charge density. We suggest that ferromagnetism may be a common occurrence at interfaces in strongly correlated situations.

So far we have applied DMFT method to a model heterostructure consisting of single-orbital Hubbard model. In reality, many correlated electron systems including transition-metal oxides have orbital degeneracy. Thus, the examination of the phase diagram of generalized model represented by multi-orbital Hubbard model using beyond Hartree-Fock techniques is an urgent task. Furthermore, the combination of DMFT and the first principle method to investigate the effect of the lattice distortions on the stability of spin and orbital orderings in the heterostructure is important future direction.

We acknowledge fruitful discussions with G. Kotliar, P. Sun, and J. Chakhalian. This research was supported by JSPS (S.O.) and the DOE under Grant No. ER 46169 (A.J.M.).

---

\* Electronic address: okapon@phys.columbia.edu

- [1] M. Imada, A. Fujimori, and Y. Tokura, *Rev. Mod. Phys.* **70**, 1039 (1998).
- [2] Y. Tokura and N. Nagaosa, *Science* **288**, 462 (2000).
- [3] C. H. Ahn, S. Gariglio, P. Paruch, T. Tybell, L. Antognazza, and J.-M. Triscone, *Science*, **284**, 1152 (1999).
- [4] S. Gariglio, C. H. Ahn, D. Matthey, and J.-M. Triscone, *Phys. Rev. Lett.* **88**, 067002 (2002).
- [5] A. Ohtomo, D. A. Muller, J. L. Grazul, and H. Y. Hwang, *Nature* **419**, 378 (2002).
- [6] M. Izumi, Y. Ogimoto, Y. Konishi, T. Manako, M. Kawasaki, and Y. Tokura, *Mat. Sci. Eng. B* **84**, 53 (2001) and references therein.
- [7] A. Biswas, M. Rajeswari, R. C. Srivastava, Y. H. Li, T. Venkatesan, R. L. Greene, and A. J. Millis, *Phys. Rev. B* **61**, 9665 (2000).
- [8] A. Biswas, M. Rajeswari, R. C. Srivastava, T. Venkatesan, R. L. Greene, Q. Lu, A. L. deLozanne, and A. J. Millis, *Phys. Rev. B* **63**, 184424 (2001).
- [9] M. Potthoff and W. Nolting, *Phys. Rev. B* **60**, 7834 (1999).
- [10] S. Schwieger, M. Potthoff, and W. Nolting, *Phys. Rev. B* **67**, 165408 (2003).
- [11] A. Liebsch, *Phys. Rev. Lett.* **90**, 096401 (2003).
- [12] R. Matzdorf, Z. Fang, Ismail, J. Zhang, T. Kimura, Y. Tokura, K. Terakura, and E. W. Plummer, *Science* **289**, 746 (2000).
- [13] M. Potthoff and W. Nolting, *Phys. Rev. B* **52**, 15341 (1995).
- [14] Z. Fang, I. V. Solovyev, and K. Terakura, *Phys. Rev. Lett.* **84**, 3169 (2000).
- [15] A. Georges, B. G. Kotliar, W. Krauth, and M. J. Rozenberg, *Rev. Mod. Phys.* **68**, 13 (1996).
- [16] S. Okamoto and A. J. Millis, *Nature (London)* **428**, 630; *Phys. Rev. B* **70**, 075101 (2004).
- [17] S. Okamoto and A. J. Millis, *Phys. Rev. B* **70**, 241104(R) (2004).

- [18] M. Potthoff, Phys. Rev. B **64**, 165114 (2001).
- [19] S. Okamoto, A. Fuhrmann, A. Comanac, and A. J. Millis, cond-mat/0502067; Phys. Rev. B (to be published).
- [20] P. J. H. Denteneer and M. Blaauboer, J. Phys.: Condens. Matter **7**, 151 (1995).